buildings

MDPI

Article

Comparison of the Use of Excavated Soil Recycled Fine Aggregate as a Substitute for River Sand in Mortar Mixing

Rong Xu [1,2] and Tong Huang [1,3,*]

[1] China Earthquake Administration, Institute of Engineering Mechanics, Harbin 150086, China; xunlu2009@126.com
[2] Earthquake Administration of Gansu Province, Lanzhou 730000, China
[3] College of Civil Engineering, Guangzhou University, Guangzhou 510145, China
* Correspondence: brasshuangtong@outlook.com

Abstract: This study comparatively investigated the performance of mortar prepared using excavated soil recycled fine aggregate (ESRFA), which mainly included fine aggregate obtained by sediment separation equipment and sieving. Scanning electron microscopy (SEM) was used to analyse the size and shape of ESRFA particles. The particle size distribution of ESRFA was uneven and its sphericality was lower than that of river sand. Two series of rendering mortar mixes were prepared using identical water/cement and aggregate/cement ratios of 0.55 and 3, respectively, using river sand as fine aggregate. ESRFA was used to replace 30%, 50%, 70%, and 100% of the river sand in each mixture. The experimental results showed that the flowability of the mortar prepared with ESRFA was lower than that of the aggregate-based mortar, but the porosity, water absorption, and mechanical properties (compressive strength, flexural strength, and drying shrinkage) increased and then decreased upon increasing the ESRFA content. In conclusion, ESRFA shows potential as a partial replacement for river sand in mortar, particularly at lower substitution rates. Further research is needed to optimize the processing and application of ESRFA in concrete to enhance its performance and sustainability.

Keywords: excavated soil; excavated soil recycled fine aggregate (ESRFA); morphological analysis; mechanical properties

check for updates

Citation: Xu, R.; Huang, T. Comparison of the Use of Excavated Soil Recycled Fine Aggregate as a Substitute for River Sand in Mortar Mixing. *Buildings* **2024**, *14*, 1917. https://doi.org/10.3390/buildings14071917

Academic Editor: Eugeniusz Koda

Received: 15 May 2024
Revised: 12 June 2024
Accepted: 19 June 2024
Published: 23 June 2024

Copyright: © 2024 by the authors. Licensee MDPI, Basel, Switzerland. This article is an open access article distributed under the terms and conditions of the Creative Commons Attribution (CC BY) license (https://creativecommons.org/licenses/by/4.0/).

1. Introduction

China is one of the world's largest consumers of sand and gravel [1,2]. Taking Guangdong Province, which has a developed economy and huge demand for sand and gravel, as an example, the consumption of sand and stone in 2020 and 2021 in the province was 1.332 billion tons and 1.345 billion tons, respectively [3]. Due to accelerated urbanization and the continuous construction of transportation infrastructure, China's demand for sand and gravel is expected to continue to increase [4]. To address this, the Chinese government is actively promoting "green mining construction," advocating for the recycling and conservation of sand and gravel, strengthening environmental protection initiatives, and promoting the sustainable use of resources [5]. Despite these efforts, construction and demolition waste is becoming an increasingly serious issue in China [6]. Construction and demolition waste includes materials such as bricks, concrete, wood, metal, glass, plastic, and excavated soil [7] that occupy land resources and pose severe environmental and public health threats [8]. China currently produces more than 3.5 billion tons of construction waste a year [9], and China's construction and demolition waste is expected to reach 7.3 billion tons by 2030 [10]. Recycling construction waste into aggregate is a promising approach to reducing the demand for raw materials and mitigating the environmental impact of construction waste [11]. However, due to recycled waste aggregate's inherent porosity, microcrack formation tendency, and high content of fine particles, recycled sand extracted from demolished building waste is an unsuitable replacement for river sand in

concrete [12,13]. Mechanical crushing, thermal treatment, and chemical treatment have been proposed to improve the performance of recycled aggregates [14], but they only marginally improve the quality of recycled sand extracted from demolished building waste. Thus, identifying suitable recycled replacements for river sand in concrete is the only viable path for achieving sustainable development in the concrete industry.

Excavated soil accounts for more than 85% of construction waste [15], but there have been few reports on its reuse, possibly because it generally requires no processing [16]. It is primarily excavated from urban and suburban areas, so its structure and composition have been altered by human activities [17,18]. Katsumi noted that excavated soil contained heavy metals, which must be considered when recycling and reusing excavated soil [19]. To recycle it, several scholars have studied the possibility of using excavated soil generated during tunnel excavation as a substitute for concrete aggregate. Grunner investigated the potential of using residual soil (mainly granite-gneiss) generated during tunnel excavation in Slovakia to completely replace quarried rock aggregate and found that aggregate derived from residual soil resulted in the lowest overall construction costs [20]. Thalmann concluded that producing high-quality concrete using aggregate from excavated residual soil was feasible and showed that 10–25% of residual soil produced by tunnel boring machine (TBM) was suitable for on-site recycling [21]. Antonaci investigated the macro-mechanical properties of concrete made from ESRFA prepared from residual soil generated in Swedish excavation projects and showed that ESRFA concrete had long-term performance comparable to that of concrete made using raw materials [22]. However, when the above results were tested in practice, Olbrecht found that processed tunnel excavation materials were similar to stone and crushed rock obtained from quarries. At higher water-to-cement ratios, this led to more significant shrinkage deformation than in traditional concrete [23]. Voit proposed washing the aggregate, adding admixtures (high-efficiency water reducers, polymer dispersants, etc.), and incorporating fibres into the concrete mixture, which improved the fracture resistance, strength, and fire resistance of concrete prepared with excavated soil recycled fine aggregate (ESRFA) [24]. Sabry Fayed improved bond performance of ribbed steel bars embedded in recycled aggregate concrete using steel mesh fabric confinement and have obtained good results [25]. Qiuying Chang predicted the Compressive Strength (CS) of ceramic waste powder concrete (CWPC) and achieved a good effect [26]. Yasin Onuralp Özkılıç removed the current sustainable complications by confirming the consumption of WFC in reinforced concrete beams (RCBs) as raw materials by experimental means [27]. Haidong Tu, using recycled sand in 3D printing, reduced the flexural stiffness and strength of the printed objects when loaded from different directions [28].

In contrast to excavated soil in Europe, which is predominantly composed of rock, excavated soil in China has a higher proportion of clay, sand, and gravel. Zhang et al. determined that excavated soil in South China is generally composed of plastic sandy clay, muddy soil, hardy sandy clay, miscellaneous fill, and medium-coarse sand. However, only 13% of excavated soil collected from subway construction sites is reused for backfilling and temporary storage for landscaping [29]. Construction projects in the Guangdong-Hong Kong-Macao Greater Bay Area have resulted in a widespread shortage of river sand in China's Pearl River Delta region [30]. Shenzhen requires approximately 50 million tons of construction sand annually, but it has almost no sand or gravel resources [31]. This has continually increased the market price of river sand, leading people to seek alternatives [32]. However, using sea sand is problematic due to chloride ion-induced steel bar rusting [33]. The concrete industry does not favour machine-made sand because of its poor workability and high micro-powder content [34]. Therefore, extracting recycled sand from excavated soil, which mainly contains silicon dioxide and aluminium oxide, similar to recycling aggregate from demolished concrete waste, has become a viable alternative for producing concrete products [35]. Recycling and reusing excavated soil to produce ESRFA can address the environmental issues related to excavated soil and minimize river sand consumption by the concrete industry. This approach is being widely promoted by the Chinese government and enterprises. Figure 1 illustrates recycling companies currently

using sediment separation equipment to process excavated soil and obtain ESRFA. Figure 2 depicts the rapid growth in the market share of ESRFA from 0% to 29.4% within three years, reaching a usage of 13.1592 million tons in 2021 [36]. ESRFA extracted from excavated soil is primarily used to replace fine aggregate in concrete, but, despite the prevailing belief that ESRFA can be used as a direct substitute for river sand without further processing, no definitive answer exists as to whether it can be used in this way without producing similar problems to those caused by sea sand.

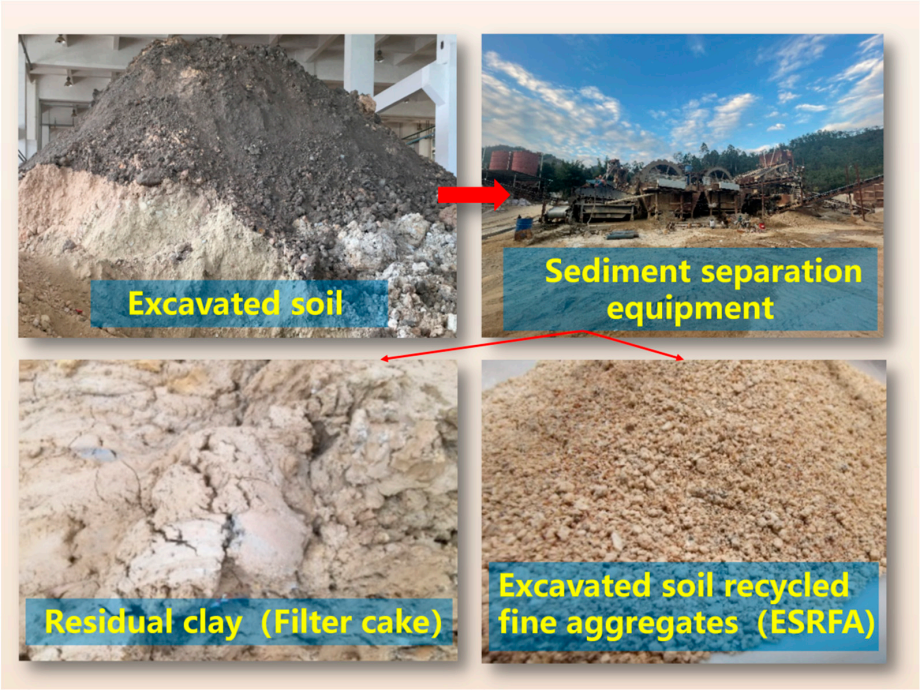


Figure 1. Separation process of ESRFA from excavated soil.

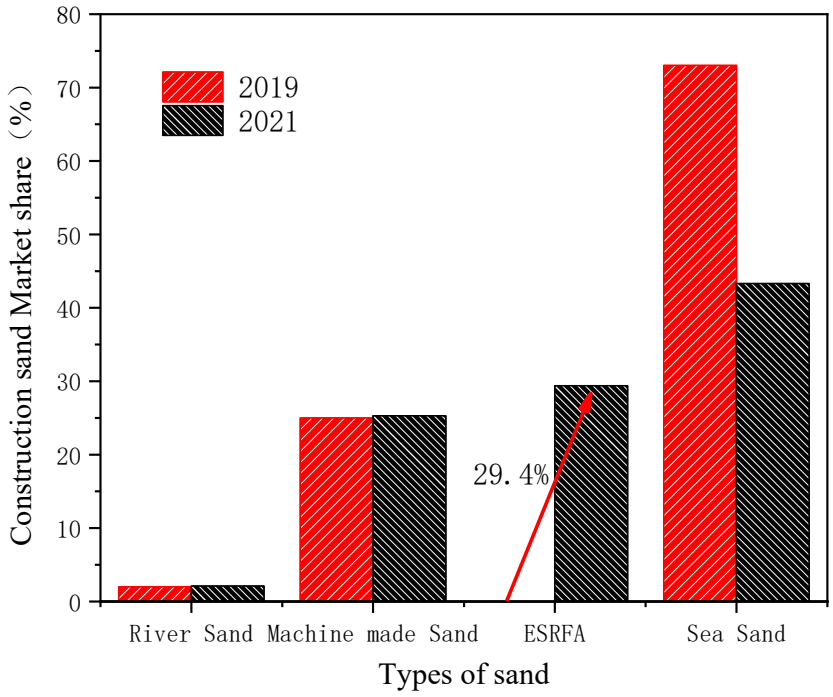


Figure 2. The market share of ESRFA and other aggregates (data from Shenzhen Housing and Construction Bureau).

To investigate the feasibility of using ESRFA as a replacement for river sand in mortar, this study investigated the application potential of recycled sand from excavated soil. The experiment was conducted in three parts. First, the physical properties of recycled sand from excavated soil were characterized, including its macromorphology, micromorphology, chemical composition, particle size, water absorption, apparent density, bulk density, and crushing index. Second, the rheological properties of fresh mortar prepared using recycled sand from excavated soil were investigated. Finally, the impact of recycled sand from excavated soil on the hardened cement's mechanical properties (flexural strength and compressive strength) was studied at different water-to-cement ratios.

2. Experimental Procedure

2.1. Materials and Characterisation

This study investigated the properties of mortar specimens prepared using two different aggregates. The first was ESRFA, obtained from a soil recycling factory in Shenzhen, China, with an apparent density of 2605 kg/m^3, a bulk density of 1435 kg/m^3, and a silt content of 3.6%. The second was river sand obtained from local material suppliers as a reference.

The morphology of the recycled sand was examined using a scanning electron microscope (SEM; FEI QuantaTM250 FEG (FEI, Lausanne, Switzerland)), which (Figure 3) exhibited a uniform particle distribution and particle size, with a particle shape and size similar to those of river sand. ImageJ2 software was used to extract particle size and roundness parameters from the SEM images [37]. First, the images were loaded into the software and then a scale factor was applied to calibrate the image size. The images were then binarized to extract the required particle information (Figure 4). Figure 5 depicts the original and binarized images of river sand and ESRFA samples used for image analysis [38].

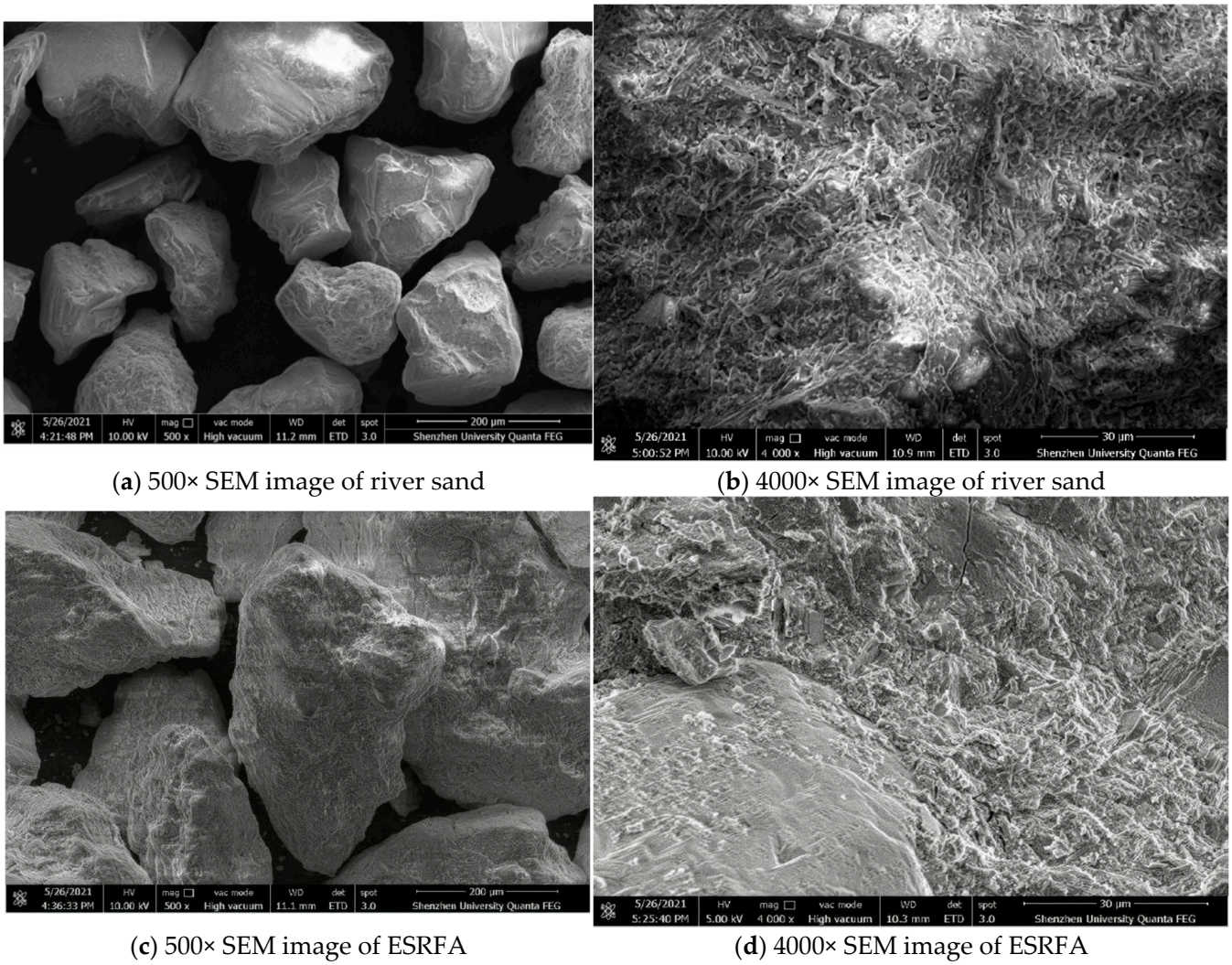


(**a**) River sand (**b**) ESRFA

Figure 3. The macroscopic appearance of ESRFA and river sand.

2.2. Mix Proportions

This study prepared two mortar mixtures, denoted Series I and Series II. Series I employed river sand as the aggregate, while Series II utilized ESAR. The cement-to-aggregate mass ratio was kept constant at 1: 3, and the water-to-cement mass ratio was kept constant at 0.55. The specific mix proportions for each series are provided in Table 1.



(**a**) 500× SEM image of river sand (**b**) 4000× SEM image of river sand

(**c**) 500× SEM image of ESRFA (**d**) 4000× SEM image of ESRFA

Figure 4. SEM images of ESRFA and river sand microstructures.

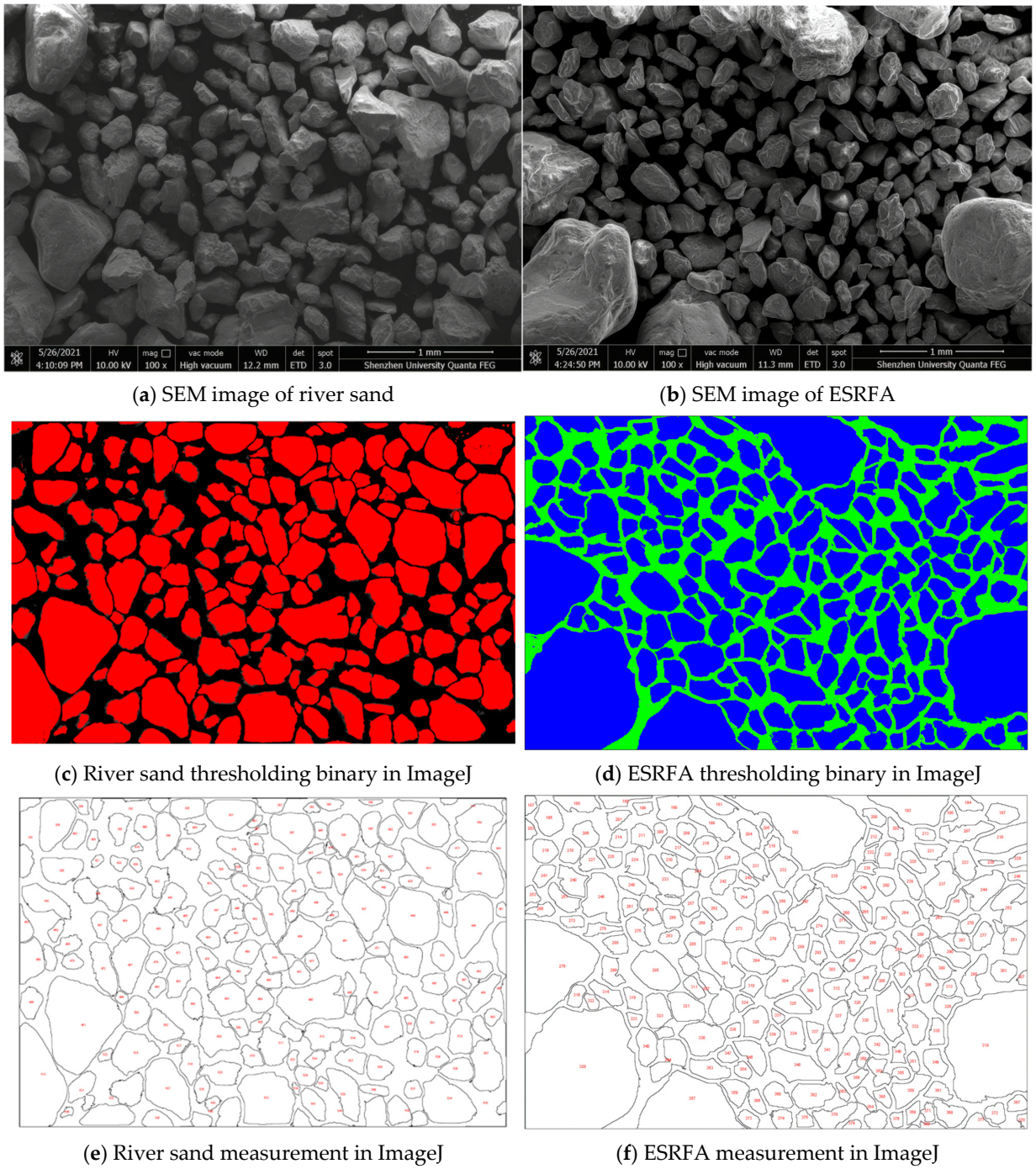
Table 1. Proportions of mortar specimens.

		Cement (g)	Water (g)	River Sand (g)	ESRFA (g)
River sand	River sand-100	150	82.5	450.0	0
ESRFA	ESRFA-10	150	82.5	405	45
	ESRFA-30	150	82.5	315	135
	ESRFA-50	150	82.5	225	225
	ESRFA-70	150	82.5	135	315
	ESRFA-100	150	82.5	0	450

2.3. Specimen Casting and Curing

The mortar mixing procedure involved adding all of the fine aggregate and water into a mixing bowl, followed by cement [39]. Initially, the fine aggregate was evenly distributed in the mixing bowl to ensure a homogeneous mixture. The precise amount of water, calculated based on the desired water-to-cement ratio, was then gradually added to the fine aggregate while continuously stirring to achieve uniform wetting. Once the fine aggregate and water were thoroughly mixed, the cement was introduced slowly to avoid clumping and to ensure even distribution. The entire mixture was then mechanically mixed at a low speed for 30 s, followed by a high-speed mix for an additional 90 s to achieve a consistent mortar paste. For each mortar mixture, 40 × 40 × 160 mm prisms were cast

and used to determine the flexural and equivalent compressive strengths, water porosity, capillary water absorption, and drying shrinkage of hardened specimens (Figure 6). The fresh mortar was carefully poured into steel molds in two layers. Each layer was compacted using a vibrating table to eliminate any entrapped air and to ensure proper consolidation of the mortar. After the second layer was added, the top surface was smoothed with a trowel to achieve a flat and even finish. The molds were then covered to prevent moisture loss and left to set. After setting for 24 h, the specimens were demolded and transferred to a water-curing tank maintained at 27 ± 1 °C. The specimens were cured in the water tank until the desired age was reached to ensure complete hydration and development of the desired mechanical properties [40].



(**a**) SEM image of river sand (**b**) SEM image of ESRFA

(**c**) River sand thresholding binary in ImageJ (**d**) ESRFA thresholding binary in ImageJ

(**e**) River sand measurement in ImageJ (**f**) ESRFA measurement in ImageJ

Figure 5. Image analysis of river sand and ESRFA.



Figure 6. Each mortar mixture generating 40 × 40 × 160 mm prisms.

2.4. Testing Procedures

2.4.1. Slump Flow

Workability needs to be evaluated to ensure the feasibility of using recycled sand in mortar [41]. The workable life of fresh mortar, initially brought to a defined flow value, was evaluated according to the Chinese standard GB/T 2419-2005 [42].

2.4.2. Porosity

Due to cement mortar's high porosity and pore connectivity, its porosity was analysed using the vacuum saturation method outlined in Chinese standard SY/T 5336-2006 [43]. Initially, prismatic samples with dimensions of 40 × 40 × 160 mm were dried in an oven at 100 ± 5 °C and their weight was measured. Then, the samples were subjected to a 12-h vacuum extraction and fully saturated by water immersion for 12 h. The porosity of the samples was determined by calculating the pore volume based on the mass difference between the dry and saturated states. To ensure accurate porosity measurements, three replicates were prepared for each sample type, and multiple measurements were taken and averaged. The porosity as a percentage is given by the equation below:

$$P = \frac{W_{\text{sat}} - W_{\text{dry}}}{W_{\text{sat}} - W_{\text{ws}}} \quad (1)$$

where P is the vacuum-saturated porosity (%); W_{sat} is the weight of air in the saturated sample; W_{ws} is the weight of water in the saturated sample; and W_{dry} is the weight of air in the oven-dried sample.

2.4.3. Water Absorption Testing

The water absorption of the specimens was tested on the 28th day of curing using specimens with the same size as those used for strength testing. Water absorption tests were conducted according to the JGJ 52-2019 Chinese standard [44] and were carried out three times, and the average values were reported. The water absorption as a percentage is given below:

$$\omega = \frac{m_{\text{ssd}} - m_{\text{d}}}{m_{\text{d}}} \quad (2)$$

where ω is the water absorption of sand (%); m_{ssd} is the mass of saturated surface-dried specimen (g); and m_d is the mass of the specimen after drying at 105 °C (g) for 24 h.

2.4.4. Strength Testing

This study employed compressive and flexural strength tests to investigate the strength of mortar specimens prepared from ESRFA. The testing procedure was carried out following Chinese standard GB/T 17671-2021 [45]. The mortar mixture was cast in 40 × 40 × 160 mm steel molds and allowed to cure for specified periods (1, 4, 7, 28, 56, and 90 days). Following the cure, mortar samples were subjected to strength tests at loading rates of 0.05 kN/s and 2.4 kN/s for flexural and compressive strength tests, respectively. The tests were conducted in triplicate, and the average values were calculated and reported (Figure 7).



Figure 7. Strength test site.

2.4.5. Drying Shrinkage

The drying shrinkage of mortar was measured according to Chinese standard JGJ/T 70-2009 [46] using cubic specimens (40 × 40 × 160 mm). The specimens were initially cured in a mold for seven days in an environment with a relative humidity exceeding 90% at 20 ± 2 °C. The molds were removed and specimens were labelled with their respective number and testing direction before being hardened in an environment with a relative humidity of 60 ± 5% at 20 ± 2 °C. Tests were conducted at specified intervals (7, 14, 21, 28, 56, and 90 days), and the drying shrinkage was calculated using Equation (1).

$$\varepsilon = \frac{L_0 - L_t}{L - L_d} \tag{3}$$

where ε is the drying shrinkage, L_0 is the initial length of the specimen, L is the length of the specimen (160 mm), L_d is the total length of the two nails buried in the specimen, and L_t is the measured length of the specimen.

3. Results and Discussion

3.1. Properties of ESRFA

With a density of 2593 kg/m^3 and a fineness modulus of 2.8, the sand was used to prepare mortar specimens. The different appearances of ESRFA and river sand are shown in Figure 3. Table 1 lists the cement's chemical composition and physical properties and the related aggregates used in this study. Portland cement (P•I42.5) was obtained from China Resources Cement Holdings Limited. The chemical composition of the recycled sand was determined by X-ray fluorescence (XRF) spectroscopy using an S4 Explorer (Bruker, Billerica, MA, USA). The XRF analysis indicated that the recycled sand had a chemical composition similar to that of river sand (Table 1), and its most abundant oxide was SiO_2 (88.5%). Other oxides detected by XRF included Al_2O_3 (8.17%), CaO (0.38%), Fe_2O_3 (0.78%), and MgO (0.184%).

Before carrying out the CO_2 curing, the apparent density and water absorption of each kind of RA were determined according to BS EN 1097-6 [47], the results of which are tabulated in Table 2. Additionally, the porosity values of the RA (p) were determined as a ratio of pore volume (Vp) to the bulk volume of the RA (V):

Table 2. Chemical composition and physical properties of the materials.

	Component	Excavated Soil (%)	River Sand (%)	ESRFA (%)	Cement (%)
Chemical composition	SiO_2	58.9	97.27	88.5	21.5
	CaO	0.636	0.23	0.38	58.81
	Al_2O_3	31.5	1.08	8.17	8.33
	Fe_2O_3	3.69	0.63	0.78	3.88
	MgO	0.596	0.13	0.184	2.67
	K_2O	2.5	0	1.17	0.752
	SO_3	0.29	0	0.05	3.24
	Cr_2O_3		0.049	0.059	
	NiO		0.021	0.019	
	MnO		0.005	0.006	
	LOI	-	-	-	2.61
Physical properties	Apparent density	-	2593 ± 100 kg/m^3	2605 ± 100 kg/m^3	-
	Bulk density	-	1498 ± 50 kg/m^3	1435 ± 50 kg/m^3	1540 ± 50 kg/m^3
	Water absorption	-			

3.2. Micromorphology and Shape Analysis

The morphology of ESRFA and river sand was assessed using SEM (Figure 3). Some fine particles enveloped the surface of the ESRFA aggregate, leading to a surface that was rougher than that of river sand. At a magnification of 4000×, many microcracks were observed within ESRFA.

The images of river sand and ESRFA particles were obtained using SEM. Their size and roundness were evaluated and compared using ImageJ2 software, as illustrated in Figure 5 [48]. Roundness refers to the degree of regularity in the shape of the sand particles and was determined by comparing the ratio between the maximum and minimum diameters of the particles. A ratio closer to 1 indicates that the particle is more spherical, while a smaller roundness value indicates that the particle has a more cubic shape [49].

Figure 5a,b show that the particle size distribution of river sand was better and exhibited a clean surface without fine particles. In contrast, ESRFA showed an inferior particle size distribution, characterized by a shortage of intermediate-sized particles, which produced an uneven distribution.

The average roundness of ESRFA was 0.6035, while that of river sand was 0.643, indicating a 6.55% higher sphericity coefficient for river sand (Figure 8). In Section 3.2, the flowability of river sand mortar was superior to ESRFA mortar with the same mix proportion because river sand's particles showed a more spherical morphology. Analysis

of the relationship between roundness and particle size revealed no significant correlation. Figure 9 shows the proportion of particles in both types of sand, which indicated a more uniform particle size distribution for river sand and a concentration of particle sizes in the 0.5–1 mm range for ESRFA, accounting for 67% of all particles. In contrast, river sand showed only 52.8% of particles in this range. In ESRFA, particles with sizes between 0.25 mm and 0.5 mm accounted for only 3% of the total, while the corresponding value for river sand was 12.4%. This difference may have been due to the artificial screening and discarding of ESRFA particles in this size range by the excavated soil recycling company to reduce the clay content in the sand.

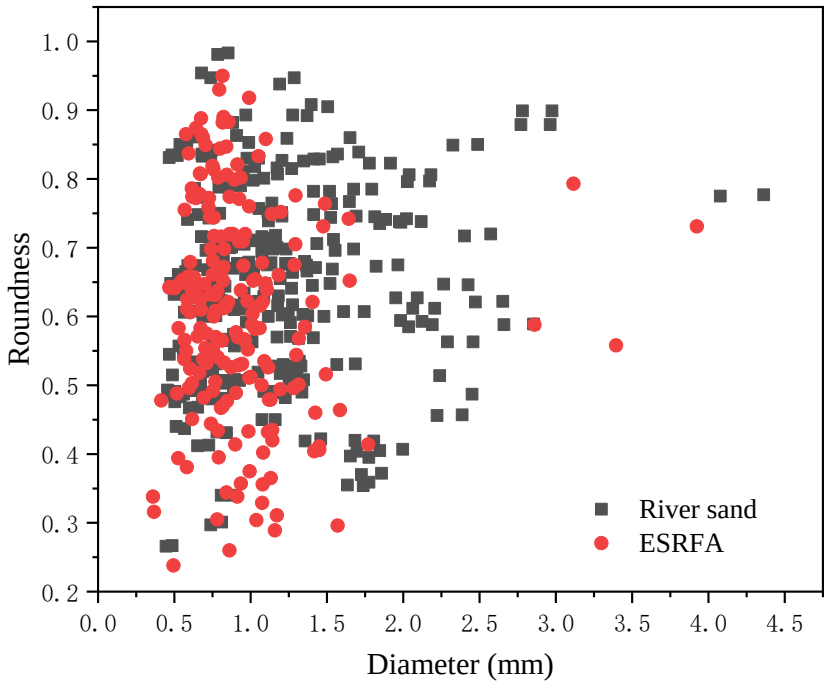


Figure 8. The roundness-particle size relationship of the two types of sand.

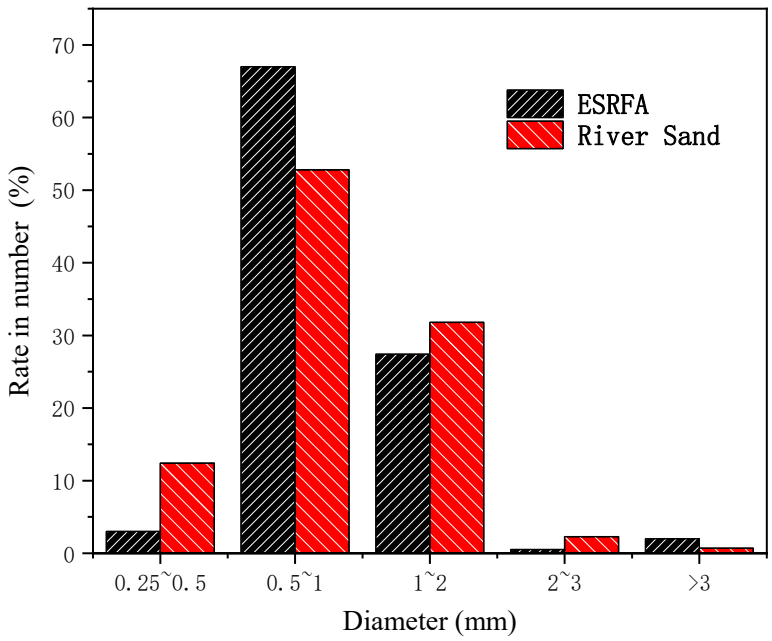


Figure 9. Particle size distributions of the two types of sand.

3.3. Properties of Fresh Mortar

Figure 10 presents the results of the flowability tests of ESRFA. The flow diameter of the mortar mixtures varied between 175 mm and 166 mm as the replacement rate of ESRFA changed. Upon increasing the replacement rate of ESRFA for river sand, the flow diameter of the mortar mixtures gradually decreased. Below or equal to a replacement rate of 30%, the flowability decrease was insignificant, but it began to increase significantly when the replacement rate of ESRFA reached 50%. When the replacement rate of ESRFA reached 100%, the flowability of the mortar mixtures was 5.14% lower than that of river sand. During mixing and testing, the workability of fresh mortar was closely related to the water absorption of the aggregate, and no bleed or segregation were observed.

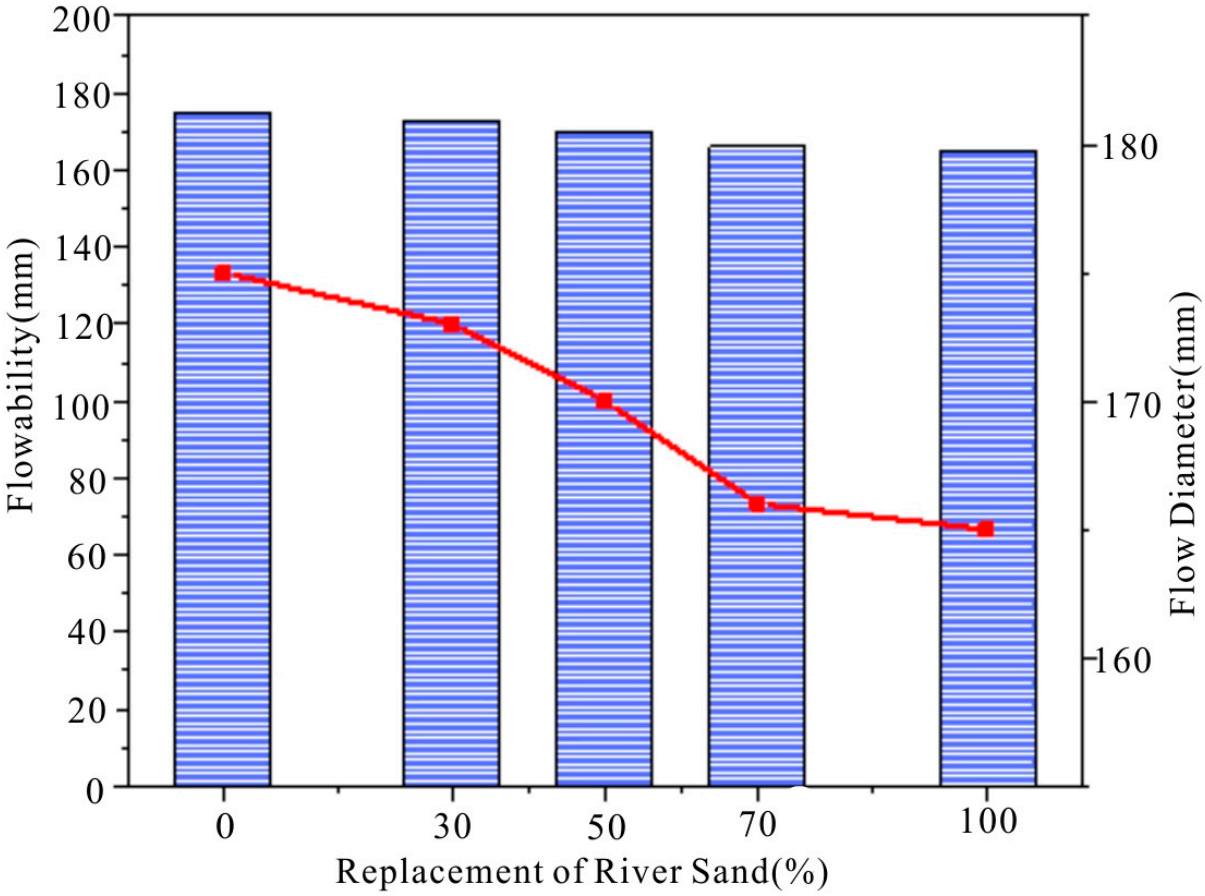


Figure 10. Flowability of mortars for ESRFA with different replacement rates.

3.4. Physical Properties of Hardened Mortar

3.4.1. Density

Figure 11 shows the density of mortars up to a substitution rate of 30% for ESRFA. The apparent density of mortar increased and eventually surpassed that of mortar made solely from river sand. This was attributed to the large particles (>3 mm) and the high content of 0.5–1 mm particles carried by ESRFA, which enhanced the aggregate skeleton. However, as the substitution rate further increased, the density of the ESRFA mortar began to decrease due to the uneven distribution of the ESRFA, which impeded the formation of a compact skeleton within the mortar. The gradual decrease in the river sand content prevented finer particles in the river sand aggregate gradation from filling these voids. Consequently, upon increasing the substitution rate of ESRFA for river sand, the apparent density of the resulting mortar gradually decreased.

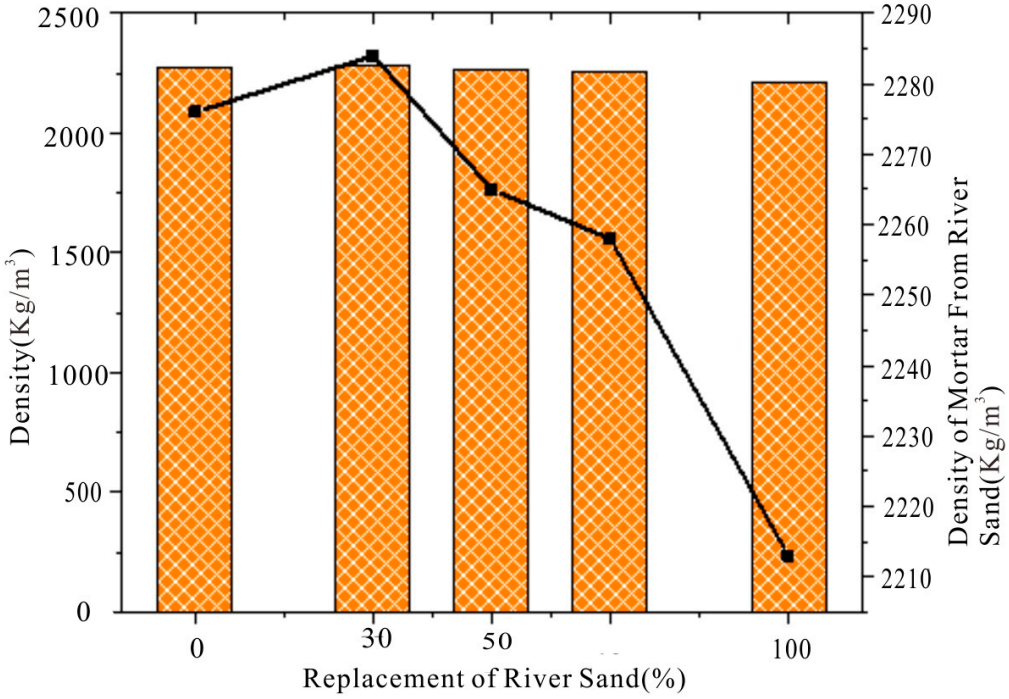


Figure 11. Density of mortars for ESRFA with different replacement ratios.

3.4.2. Porosity of the Mortars

Figure 12 illustrates the relationship between the ESRFA replacement rate and mortar porosity. Above a 30% replacement rate, the porosity of mortar gradually increased because the aggregate affected the internal structure of the mortar. When ESRFA replaced about 30% of river sand in mortar, although the flowability decreased, the flexural and compressive strengths, porosity, water absorption, and dry shrinkage all increased. Furthermore, as the replacement rate of ESRFA increased, the clay content in the mortar also increased, which absorbed reactive water. This slowed or even inhibited the hydration reaction of the mortar, which decreased its compactness and increased its porosity.

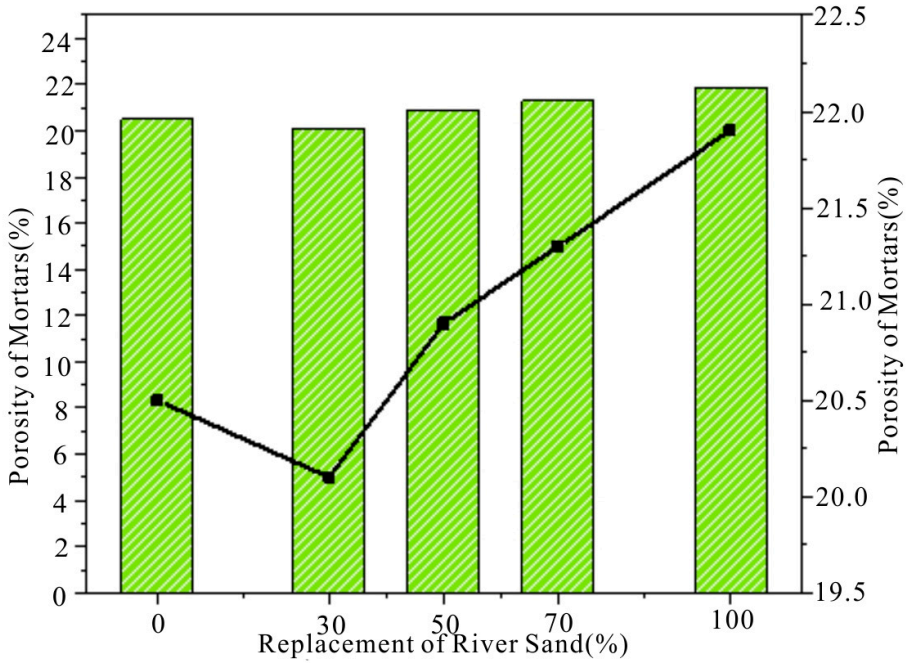


Figure 12. Porosity of mortars for ESRFA with different replacement ratios.

3.4.3. Water Absorption

Table 3 presents the water absorption values of mortar, in which at an ESRFA replacement rate of 30%, the water absorption rate decreased by 1.4%. However, as the replacement rate continued to increase to 50%, 70%, and 100%, the water absorption rate increased by 2.59%, 5.63%, and 8.03%, respectively, relative to river sand mortar. These results were attributed to the non-uniform particle size distribution of ESRFA. As the ESRFA replacement rate increased, the compactness of the mortar decreased, which increased the internal porosity of the mortar and thus increased its water absorption rate.

Table 3. Water absorption percent of hardened mortars.

	River Sand-100	ESRFA-30	ESRFA-50	ESRFA-70	ESRFA-100
Mean, %	12.12	11.95	12.43	12.82	13.15
Std Dev	0.38	0.25	0.33	0.29	0.21

3.5. Mechanical Properties of Hardened Mortar

3.5.1. Compressive and Flexural Strengths

Figures 13 and 14 illustrate the evolution of the flexural and compressive strengths of mortar samples over 90 days. Table 4 presents the corresponding flexural and compressive strengths. The results reveal that for a given curing time, the flexural and compressive strengths initially increased and then decreased upon increasing the ESRFA content. When the ESRFA substitution rate for river sand was 30%, the flexural and compressive strength were higher than those of mortar using only river sand at 28 days, representing increases of 6.74% and 3.32%, respectively, and 4.12% and 1.15% at 90 days (Figure 13). When the ESRFA substitution rate for river sand was 100%, the mortar's flexural and compressive strengths were higher than those of the river sand mortar, representing decreases of 10.11% and 10.46% at 28 days, respectively, and decreases of 8.55% and 11.34% at 90 days (Figure 14.).

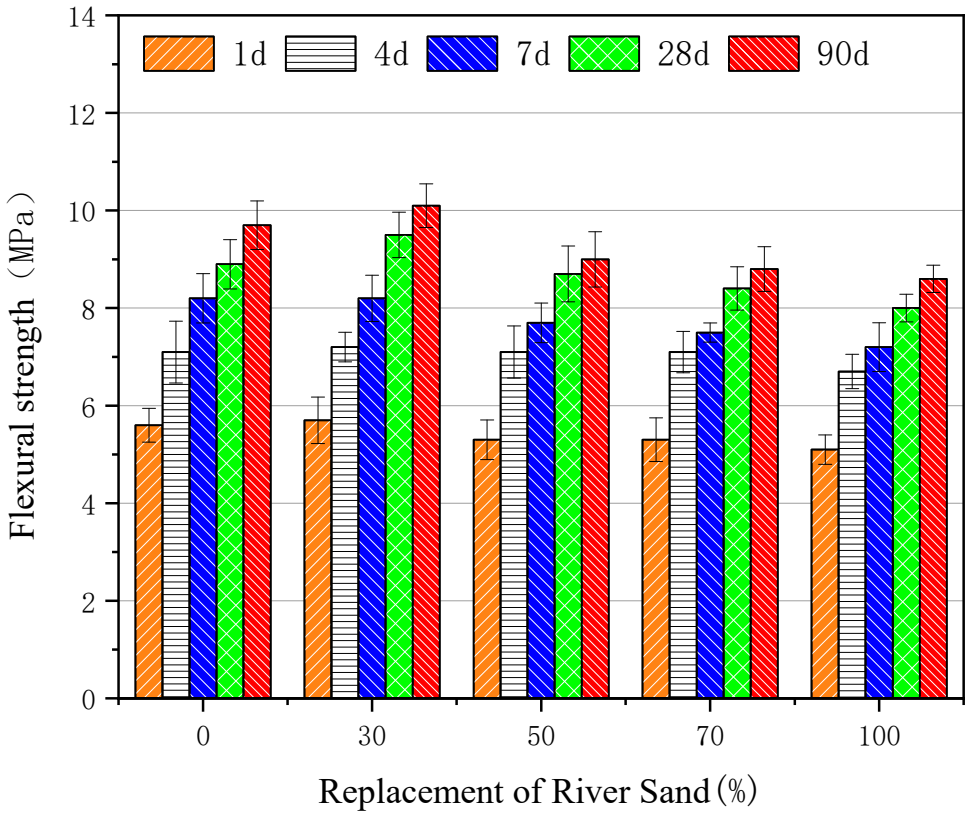


Figure 13. Flexural strength of mortars using ESRFA with different replacement rates.

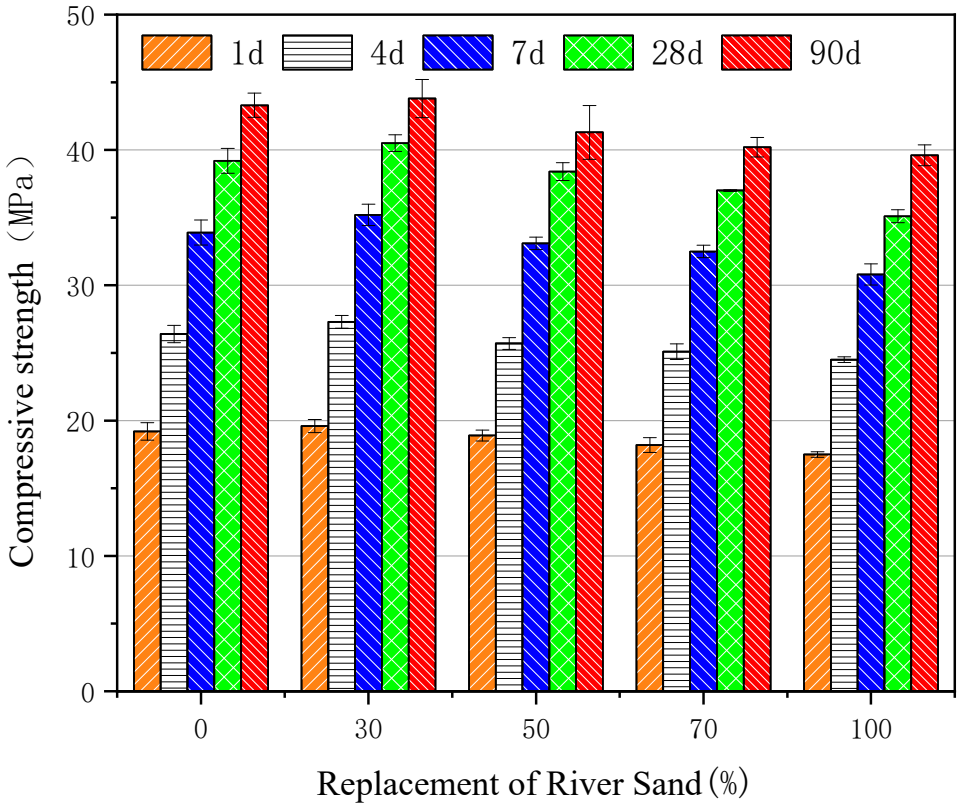


Figure 14. Compressive strength of mortars for ESRFA with different replacement rates.

Table 4. Relative flexural and compressive strength of mortar.

		1 d	3 d	7 d	28 d	56 d
Flexural strength	River sand-100	5.6	7.1	8.2	8.9	9.7
	ESRFA-30	5.7	7.2	8.2	9.5	10.1
	ESRFA-50	5.3	7.1	7.7	8.7	9.0
	ESRFA-70	5.3	7.1	7.5	8.4	8.8
	ESRFA-100	5.1	6.7	7.2	8.0	8.6
Compressive strength	River sand-100	19.2	26.4	33.9	39.2	43.3
	ESRFA-30	19.6	27.3	35.2	40.5	43.8
	ESRFA-50	18.9	25.7	33.1	38.4	41.3
	ESRFA-70	18.2	25.1	32.5	37.0	40.2
	ESRFA-100	17.5	24.5	30.8	35.1	39.6

At 28 days, the flexural strengths of specimens with ESRFA replacement rates of 30%, 50%, 70%, and 100% were, respectively, 66.67%, 64.15%, 58.49%, and 56.86% higher than those on day one. Similarly, the compressive strength of specimens with ESRFA replacement rates of 30%, 50%, 70%, and 100% were, respectively, 106.63%, 103.17%, 103.30%, and 100.57% higher than those on day one. However, no filling effect or acceleration in the strength increase was observed during the early curing period upon increasing the ESRFA substitution rate in the mortar (Figure 15).

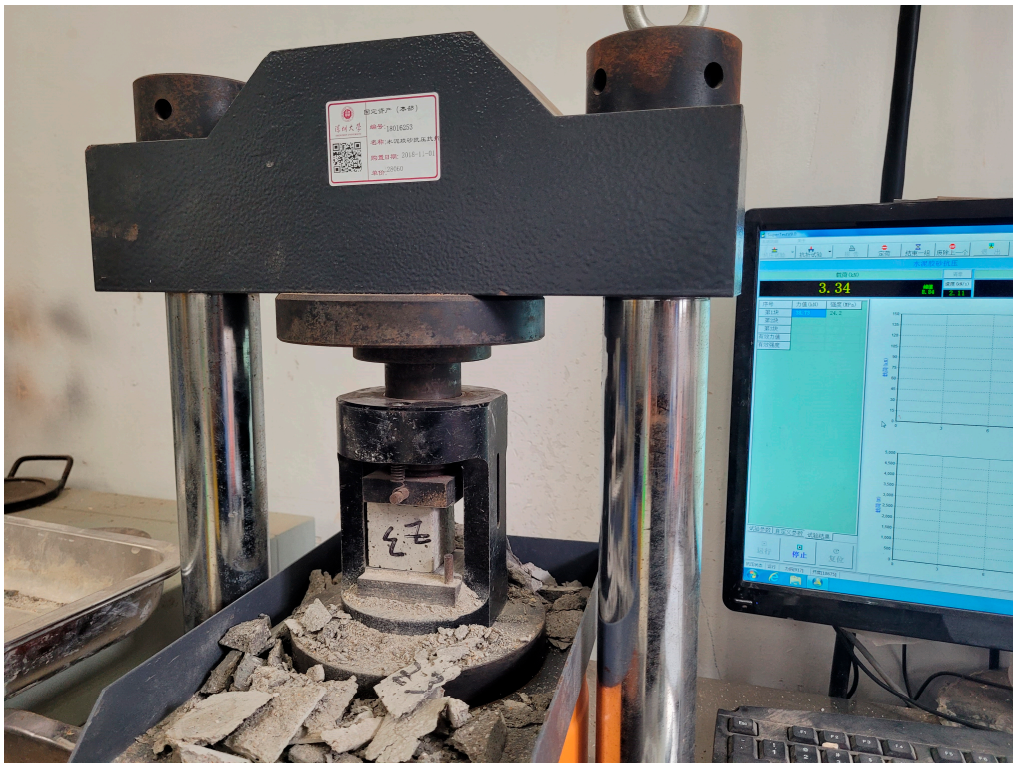


Figure 15. Rupture in strength test.

At 90 days, the flexural strength of specimens with ESRFA replacement rates of 30%, 50%, 70%, and 100% were, respectively, 6.32%, 3.45%, 4.76%, and 7.50% higher than those at 28 days. Furthermore, the compressive strengths of specimens with ESRFA replacement rates of 30%, 50%, 70%, and 100% were, respectively, 8.15%, 7.55%, 8.65%, and 12.82% higher than those at 28 days. The flexural and compressive strengths showed a non-linear relationship upon increasing the ESRFA content and were characterized by an initial increase followed by a decrease.

3.5.2. Drying Shrinkage Rate of ESRFA Mortars

Figure 16 shows that the drying shrinkage rate of ESRFA mortars is different at different substitution rates, in which the mortar with 100% ESRFA had the highest drying shrinkage. The drying shrinkage of mortars with ESRFA aggregate contents of 50%, 70%, and 100% content showed increases of 9.0%, 21.9%, and 27.5%, respectively, after 90 days compared with mortars without ESRFA. These results showed that the dry shrinkage increase rate upon ESRFA addition is less marked beyond 50% addition of ESRFA. Specifically, the shrinkage rate of ESRFA-50 increased by 11.59% compared with ESRFA-30, whereas the shrinkage rate of ESRFA-70 increased by 11.85% compared with ESRFA-50, and the shrinkage rate of ESRFA-100 increased by only 4.62% compared with ESRFA-70. However, when the ESRFA content increased to 30%, the 90-day drying shrinkage decreased by 2.49%. Some ESRFA containing coarse and fine particles enhanced the skeleton effect of the mortar, giving the aggregate inside the mortar a uniform particle size distribution, thus reducing its drying shrinkage.

Mesbah and Buyle-Bodin found that mortar specimens showed more considerable drying shrinkage due to their higher porosity and water absorption [50]. The influence of ESRFA on the drying shrinkage of hardened specimens was ascribed to three factors: (1) porosity, (2) water absorption, and (3) clay content. It is widely recognized that the primary mechanism responsible for drying shrinkage is the loss of moisture from mortar, which is maintained by capillary tension in the hydrated cement paste's pores and is lost via physically adsorbed water in the C-S-H gel [51]. Therefore, the drying shrinkage of

hardened specimens was closely linked to mortar's water absorption, which is tabulated in Table 3. The results reveal a non-linear trend in which the water absorption initially decreased before increasing as the ESRFA content was increased. The clay content in mortar prepared using ESRFA sequestered a portion of the free water in the mixing water by the clay, which prevented it from being consumed by cement hydration reactions.

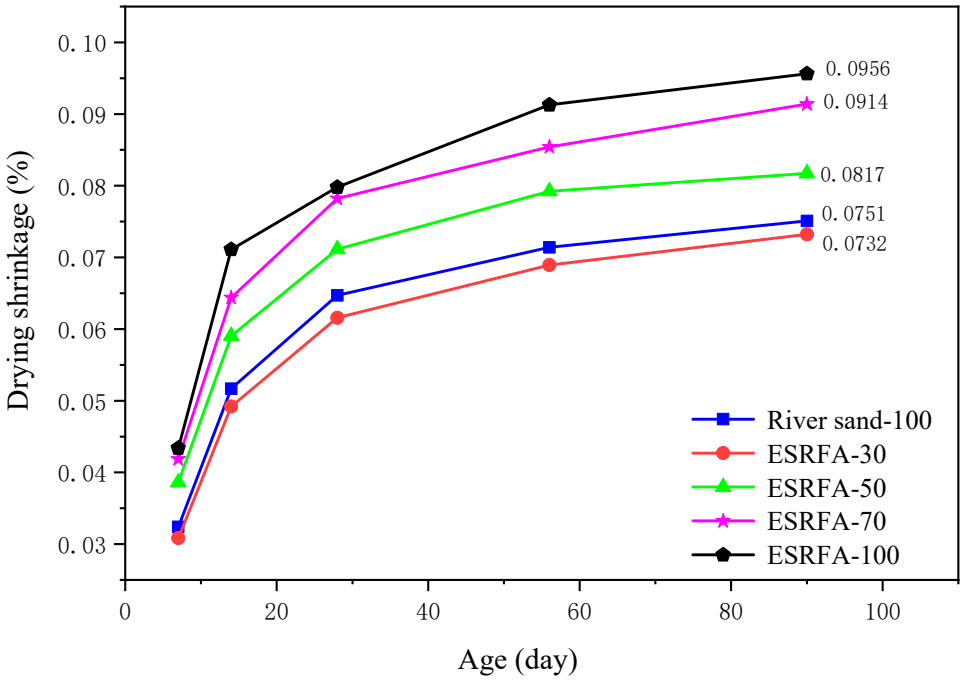


Figure 16. Drying shrinkage of mortars.

Consequently, the drying shrinkage of the resulting mortar specimens increased due to the evaporation of water absorbed by the clay during the later stages of hardening. Additionally, the absolute clay content in the mortar underwent a marked increase upon progressively increasing the ESRFA substitution rate. This increase in clay content exacerbated the dry shrinkage of the mortar, which accounted for the trend in which the drying shrinkage first decreased to 2.49% and then increased to 27.5% upon increasing the ESRFA content.

4. Conclusions

This study explored the feasibility of using ESRFA to replace river sand as an aggregate during mortar preparation. Based on the results obtained, the following conclusions can be drawn:

- Micromorphology and shape analysis revealed that the roundness coefficient of river sand was 6.55% higher than ESRFA. This was reflected in the flowability test of the mortar, where river sand mortar exhibited superior flowability to ESRFA mortar because; when the surface of aggregate particles was more cubic and rougher, they significantly reduced the workability of fresh mortar by increasing the resistance to particle sliding. In addition, river sand exhibited a more uniform particle size distribution than ESRFA, which showed a greater particle size concentration, with 67% of the particles distributed between 0.5 mm and 1 mm. Thus, modifying the uniformity of particle size distribution is a plausible strategy for enhancing the replacement rate of aggregates in mortar.
- The flexural and compressive strength, porosity, water absorption, and dry shrinkage of mortar increased and then decreased upon increasing the ESRFA content.
- When ESRFA replaced about 30% of river sand in mortar, although the flowability decreased, the flexural and compressive strengths, porosity, water absorption, and

dry shrinkage all increased. Therefore, the reasonable use of ESRFA during mortar mixing may enhance its performance, but adding ESRFA will decrease the fluidity of mortar, regardless of the mixing ratio. Therefore, the improvement of the workability of ESRFA cement products should be considered during use.

- The experimental results showed that ESRFA could be used to partly replace river sand during the production of cement products and had good physical properties.
- Using ESRFA helps address the environmental issues associated with excavated soil disposal and reduces the reliance on river sand, offering a sustainable alternative for the concrete industry.
- Overall, ESRFA can be a viable partial replacement for river sand in mortar, particularly at substitution rates up to 30%, providing economic and environmental benefits without compromising the mechanical properties of the mortar.

Author Contributions: Writing—original draft, R.X.; Writing—review & editing, T.H. All authors have read and agreed to the published version of the manuscript.

Funding: We thanks for the fund supported by Special Fund for Innovation Team, Gansu Earthquake Agency (2019TD-02-01); Science and technology plan project in Gansu Province (22JR5RA821); Earthquake Tracking and Directional Work Task for 2024 (2024010105).

Data Availability Statement: The original contributions presented in the study are included in the article, further inquiries can be directed to the corresponding authors.

Conflicts of Interest: The authors declare no conflict of interest.

Abbreviations

ESRFA: excavated soil recycled fine aggregates; SEM: Scanning electron microscopy; XRF: X-ray fluorescence

References

1. Wang, W.; Jiang, D.; Chen, D.; Chen, Z.; Zhou, W.; Zhu, B. A Material Flow Analysis (MFA)-based potential analysis of eco-efficiency indicators of China's cement and cement-based materials industry. *J. Clean. Prod.* **2016**, *112*, 787–796. [CrossRef]
2. de Leeuw, J.; Shankman, D.; Wu, G.; de Boer, W.F.; Burnham, J.; He, Q.; Yesou, H.; Xiao, J. Strategic assessment of the magnitude and impacts of sand mining in Poyang Lake, China. *Reg. Environ. Chang.* **2010**, *10*, 95–102. [CrossRef]
3. Zhang, Y.; Liang, F.; Zhang, S. Research on Current Supply and Demand Situation and Trend of Sandstone on Guangdong Province. *World Build. Mater.* **2024**, *42*, 80–86.
4. Huang, T.; Kou, S.; Liu, D.; Li, D.; Xing, F. Evaluation of the Techno-Economic Feasibility for Excavated Soil Recycling in Shenzhen, China. *Sustainability* **2022**, *14*, 3028. [CrossRef]
5. Li, S.; Yu, L.; Jiang, W.; Yu, H.; Wang, X. The recent progress China has made in green mine construction, Part I: Mining groundwater pollution and sustainable mining. *Int. J. Environ. Res. Public Health* **2022**, *19*, 5673. [CrossRef] [PubMed]
6. Duan, H.; Li, J. Construction and demolition waste management: China's lessons. *Waste Manag. Res.* **2016**, *34*, 397–398. [CrossRef] [PubMed]
7. Poon, C.S.; Ann, T.W.; Ng, L.H. On-site sorting of construction and demolition waste in Hong Kong. *Resour. Conserv. Recycl.* **2001**, *32*, 157–172. [CrossRef]
8. Ziraba, A.K.; Haregu, T.N.; Mberu, B. A review and framework for understanding the potential impact of poor solid waste management on health in developing countries. *Arch. Public Health* **2016**, *74*, 54. [CrossRef]
9. Zhang, Y. Development Situation of Construction Waste Treatment Industry. *Recycl. Resour. Circ. Econ.* **2023**, *16*, 22–24.
10. Wang, Y. Low Utilization Rate of Construction Waste Recycling, Experts Suggest Improving Special Legislation. *Resour. Recycl.* **2020**, *9*, 10–12.
11. Yang, J.; Du, Q.; Bao, Y. Concrete with recycled concrete aggregate and crushed clay bricks. *Constr. Build. Mater.* **2011**, *25*, 1935–1945. [CrossRef]
12. Song, X.; Qiao, P.; Wen, H. Recycled aggregate concrete enhanced with polymer aluminium sulfate. *Mag. Concr. Res.* **2015**, *67*, 496–502. [CrossRef]
13. 0Vijay, K.; Murmu, M.; Deo, S.V. Bacteria based self healing concrete—A review. *Constr. Build. Mater.* **2017**, *152*, 1008–1014. [CrossRef]
14. Purushothaman, R.; Amirthavalli, R.R.; Karan, L. Influence of treatment methods on the strength and performance characteristics of recycled aggregate concrete. *J. Mater. Civ. Eng.* **2015**, *27*, 04014168. [CrossRef]

15. Li, Y. *Developing a Sustainable Construction Waste Estimation and Management System*; Hong Kong University of Science and Technology (Hong Kong) ProQuest Dissertations Publishing: Hong Kong, China, 2013; p. 3613928.
16. Singh, A.; Kuhad, R.C.; Ward, O.P. Biological remediation of soil: An overview of global market and available technologies. In *Advances in Applied Bioremediation*; Springer: Berlin/Heidelberg, Germany, 2009; pp. 1–19. [CrossRef]
17. Van Veen, J.A.; Kuikman, P.J. Soil structural aspects of decomposition of organic matter by micro-organisms. *Biogeochemistry* **1990**, *11*, 213–233. [CrossRef]
18. Geisen, S.; Wall, D.H.; van der Putten, W.H. Challenges and opportunities for soil biodiversity in the anthropocene. *Curr. Biol.* **2019**, *29*, R1036–R1044. [CrossRef] [PubMed]
19. Katsumi, T. *Towards Sustainable Soil Management-Reuse of Excavated Soils with Contamination*; Environmental Science and Engineering; Springer: Singapore, 2018; pp. 99–118. [CrossRef]
20. Grünner, K.; Durmeková, T.; Wagner, P. Exploitation possibilities of the tunnel's muck as a construction material. *Slovak J. Civ. Eng.* **2003**, *1*, 11–25. Available online: https://www.svf.stuba.sk/buxus/docs/sjce/2003/2003_1/file2.pdf (accessed on 16 August 2004).
21. Thalmann-Suter, C.N. Concrete Aggregate Production with TBM Muck Explained on the AlpTransit Tunnel Projects. In *Utilizing Ready Mix Concrete and Mortar*; Dhir, R.K., Limbachiya, M.C., Eds.; Thomas Telford: London, UK, 1999; pp. 131–144.
22. Antonaci, P.; Masera, D. Mechanical Behavior of Structural Concrete Made with Recycled Aggregates from Tunnel Excavation. In *Key Engineering Materials*; Trans Tech Publications Ltd.: Stafa-Zurich, Switzerland, 2011; Volume 452. [CrossRef]
23. Olbrecht, H.; Studer, W. Use of TBM chip as concrete aggregate. *Mater. Struct.* **1998**, *31*, 184–187. Available online: https://www.dora.lib4ri.ch/empa/islandora/object/empa:4126/datastream/PDF/Olbrecht-1998-Use_of_TBM_chips_as-(published_version).pdf (accessed on 14 May 2024). [CrossRef]
24. Voit, K.; Kuschel, E. Rock material recycling in tunnel engineering. *Appl. Sci.* **2020**, *10*, 2722. [CrossRef]
25. Fayed, S.; Madenci, E.; Özkiliç, Y.O.; Mansour, W. Improving bond performance of ribbed steel bars embedded in recycled aggregate concrete using steel mesh fabric confinement. *Constr. Build. Mater.* **2023**, *369*, 130452. [CrossRef]
26. Chang, Q.; Liu, L.; Farooqi, M.U.; Thomas, B.; Özkılıç, Y.O. Data-driven based estimation of waste-derived ceramic concrete from experimental results with its environmental assessment. *J. Mater. Res. Technol.* **2023**, *24*, 6348–6368. [CrossRef]
27. Özkılıç, Y.O.; Başaran, B.; Aksoylu, C.; Karalar, M.; Martins, C.H. Mechanical behavior in terms of shear and bending performance of reinforced concrete beam using waste fire clay as replacement of aggregate. *Case Stud. Constr. Mater.* **2023**, *18*, e02104. [CrossRef]
28. Tu, H.; Wei, Z.; Bahrami, A.; Kahla, N.B.; Ahmad, A.; Özkılıç, Y.O. Recent advancements and future trends in 3D printing concrete using waste materials. *Dev. Built Environ.* **2023**, *16*, 100187. [CrossRef]
29. Zhang, N.; Duan, H.; Sun, P. Characterizing the generation and environmental impacts of subway-related excavated soil and rock in China. *J. Clean. Prod.* **2020**, *248*, 119242. [CrossRef]
30. Bie, J.; de Jong, M.; Derudder, B. Greater Pearl River Delta: Historical evolution towards a global city-region. *J. Urban Technol.* **2015**, *22*, 103–123. [CrossRef]
31. Bao, Z.; Lu, W. Developing efficient circularity for construction and demolition waste management in fast emerging economies: Lessons learned from Shenzhen, China. *Sci. Total Environ.* **2020**, *724*, 138264. [CrossRef] [PubMed]
32. Bhatawdekar, R.M.; Singh, T.N.; Tonnizam Mohamad, E.; Armaghani, D.J.; Binti Abang Hasbollah, D.Z. River sand mining vis a vis manufactured sand for sustainability. In *Proceedings of the International Conference on Innovations for Sustainable and Responsible Mining: ISRM 2020*; Springer International Publishing: Cham, Switzerland, 2021; Volume 1. [CrossRef]
33. Jiao, S.J.; Wang, S. Utilizing Sea Sand in Construction. In *Advanced Materials Research*; Trans Tech Publications Ltd.: Stafa-Zurich, Switzerland, 2014; Volume 838.
34. He, H.; Wang, Y.; Wang, J. Compactness and hardened properties of machine-made sand mortar with aggregate micro fines. *Constr. Build. Mater.* **2020**, *250*, 118828. [CrossRef]
35. Behera, M.; Bhattacharyya, S.K.; Minocha, A.K.; Deoliya, R.; Maiti, S. Recycled aggregate from C&D waste & its use in concrete–A breakthrough towards sustainability in construction sector: A review. *Constr. Build. Mater.* **2014**, *68*, 501–516. [CrossRef]
36. Shenzhen Housing and Construction Bureau, Letter from the Shenzhen Housing and Construction Bureau in response to Proposal No. 20220605 of the 7th Shenzhen Municipal People's Congress. 12 July 2022. Available online: http://zjj.sz.gov.cn/csml/bgs/xxgk/tabl_1/jybl/content/post_10310829.html (accessed on 14 May 2024).
37. Takashimizu, Y.; Iiyoshi, M. New parameter of roundness R: Circularity corrected by aspect ratio. *Prog. Earth Planet. Sci.* **2016**, *3*, 2. [CrossRef]
38. Mog, K.; Anbazhagan, P. An inexpensive foldscopic approach for quantitative evaluation of the shape of sand particles. *Curr. Sci.* **2023**, *124*, 457–466.
39. Williams, D.A.; Saak, A.W.; Jennings, H.M. The influence of mixing on the rheology of fresh cement paste. *Cem. Concr. Res.* **1999**, *29*, 1491–1496. [CrossRef]
40. Kou, S.-C.; Zhan, B.-J.; Poon, C.-S. Use of a CO_2 curing step to improve the properties of concrete prepared with recycled aggregates. *Cem. Concr. Compos.* **2014**, *45*, 22–28. [CrossRef]
41. Liu, Q.; Singh, A.; Xiao, J.; Li, B.; Tam, V.W. Workability and mechanical properties of mortar containing recycled sand from aerated concrete blocks and sintered clay bricks. *Resour. Conserv. Recycl.* **2020**, *157*, 104728. [CrossRef]

42. *GB/T 2419-2005*; Test Method for Fluidity of Cement Mortar. Ministry of Housing and Urban-Rural Development of the People's Republic of China Press: Beijing, China, 2005.
43. *SY/T 5336-2006*; The Petroleum and Gas Industry Standards of China. National Energy Administration Press: Beijing, China, 2006.
44. *JGJ 52-2019*; Standard for Technical Requirements and Test Method of Sand and Crushed Stone (or Gravel) for Ordinary Concrete. Ministry of Housing and Urban-Rural Development of the People's Republic of China Press: Beijing, China, 2019.
45. *GB/T 17671-2021*; Cement Mortar Strength Testing Method (ISO). China Standards Press: Beijing, China, 2021.
46. *JGJ/T 70-2009*; Standard for test method of basic properties of construction mortar. Ministry of Housing and Urban-Rural Development of the People's Republic of China Press: Beijing, China, 2009.
47. *BS EN 1097-6:2022*; Tests for mechanical and physical properties of aggregates Determination of particle density and water absorption. British Standards Institution: London, UK, 2022.
48. Prakongkep, N.; Suddhiprakarn, A.; Kheoruenromne, I.; Gilkes, R.J. SEM image analysis for characterization of sand grains in Thai paddy soils. *Geoderma* **2010**, *156*, 20–31. [CrossRef]
49. Bahadur, S.; Badruddin, R. Erodent particle characterization and the effect of particle size and shape on erosion. *Wear* **1990**, *138*, 189–208. [CrossRef]
50. Mesbah, H.; Buyle-Bodin, F. Efficiency of polypropylene and metallic fibres on control of shrinkage and cracking of recycled aggregate mortars. *Constr. Build. Mater.* **1999**, *13*, 439–447. [CrossRef]
51. Wu, C.; Kou, S. Effects of high-calcium sepiolite on the rheological behaviour and mechanical strength of cement pastes and mortars. *Constr. Build. Mater.* **2019**, *196*, 105–114. [CrossRef]

Disclaimer/Publisher's Note: The statements, opinions and data contained in all publications are solely those of the individual author(s) and contributor(s) and not of MDPI and/or the editor(s). MDPI and/or the editor(s) disclaim responsibility for any injury to people or property resulting from any ideas, methods, instructions or products referred to in the content.